Geometrical-spreading correction for P-waves in layered azimuthally anisotropic media

Xiaoxia Xu and Ilya Tsvankin
Center for Wave Phenomena, Department of Geophysics, Colorado School of Mines, Golden, CO 80401.

ABSTRACT
Compensation for the geometrical spreading along the raypath is an essential step in AVO (amplitude variation with offset) analysis, in particular for wide-azimuth surveys. Here, we propose an efficient methodology to correct long-spread reflection data for the geometrical spreading in stratified azimuthally anisotropic media. The geometrical-spreading factor is expressed through the reflection traveltime described by the nonhyperbolic moveout equation that has the same form as that in VTI (transversely isotropic with a vertical symmetry axis) media.
For P-waves, the adapted VTI equation is parameterized by the normal-moveout (NMO) ellipse and the azimuthally varying anellipticity parameter η. If the vertical symmetry planes have uniform orientation in all layers, a close approximation to the exact traveltime can be obtained by using the expression for $\eta(\alpha)$ originally derived for a single orthorhombic layer. For models with misaligned symmetry planes, the azimuthal variation of η is described by an additional angle that controls the rotation of the "principal" axes of the function $\eta(\alpha)$ with respect to the NMO ellipse.
The moveout parameters are estimated from the 3D nonhyperbolic semblance algorithm of Vasconcelos and Tsvankin that operates simultaneously with traces at all offsets and azimuths. Numerical tests for models composed of orthorhombic layers with strong, depth-varying velocity anisotropy confirm the high accuracy of our travetime-fitting procedure and, therefore, of the geometrical-spreading correction. In the presence of azimuthal anisotropy above the reflector, the azimuthal variation of the geometrical-spreading factor is often comparable to that of the reflection coefficient.
The algorithm was applied to 3D data collected at Weyburn field (Canada) to evaluate the geometrical spreading for wide-azimuth P-wave reflections. The geometrical-spreading factor for the reflection from the top of the fractured reservoir is clearly influenced by the azimuthal anisotropy in the overburden, which should cause distortions in the azimuthal AVO attributes. Since our geometrical-spreading correction is entirely based on the kinematics of reflected arrivals, it can be readily incorporated into the processing flow of azimuthal AVO analysis.

Key words: geometrical-spreading correction, azimuthal anisotropy, wide-azimuth AVO

Introduction

Seismic signatures measured in wide-azimuth reflection surveys may be strongly influenced by azimuthal anisotropy associated with natural fracture systems or dipping transversely isotropic layers (e.g., shales). The inversion of azimuthally varying moveout velocities, polarization vectors, and amplitudes of reflected waves gives valuable information for characterization of frac-

tured reservoirs and lithology discrimination (Mallick et al., 1998; Grechka and Tsvankin, 1999a; Lynn et al., 1999; Bakulin et al., 2000; Rüger, 2001; Hall and Kendall, 2003). Although the most direct evidence of the presence of azimuthal anisotropy is provided by shear-wave splitting, estimation of a representative set of anisotropic parameters is impossible without performing azimuthal moveout and AVO (amplitude variation with offset) analysis.

The main advantages of the anisotropic AVO inversion is its potential to resolve the reflection coefficient at the target horizon and the high sensitivity of body-wave amplitudes to the anisotropic parameters (e.g., Tsvankin, 1995; 2001). However, the transformation of seismic amplitudes measured at the surface into the reflection coefficients involves the corrections for the source signature and propagation phenomena along the raypath (e.g., Maultzsch et al., 2003). Major amplitude distortions in anisotropic media, in particular for wide-azimuth data, are caused by the directionally varying geometrical spreading above the reflector. A detailed discussion of geometrical spreading in TI and orthorhombic media can be found in Tsvankin (2001, Chapter 2) and Xu et al. (2003; hereafter referred to as Paper I).

If the velocity model of the overburden is known, the geometrical-spreading correction can be accomplished by applying dynamic ray tracing. A more practical approach, however, is based on expressing geometrical spreading through reflection traveltimes. As shown in Paper I the geometrical-spreading factor L at the surface can be found as the following function of the traveltime T:

$$L(x,\alpha) = \frac{\sqrt{\cos\phi^s \cos\phi^r}}{V_g} \left[\frac{\partial^2 T}{\partial x^2}\frac{\partial T}{\partial x}\frac{1}{x} + \frac{\partial^2 T}{\partial x^2}\frac{\partial^2 T}{\partial \alpha^2}\frac{1}{x^2} - \left(\frac{\partial T}{\partial \alpha}\right)^2 \frac{1}{x^4}\right]^{-1/2}, \quad (1)$$

where x is the source-receiver offset, α is the azimuth of the source-receiver line with respect to the x_1-axis, V_g is the group velocity at the source location, and ϕ^s and ϕ^r are the angles between the ray and the vertical at the source and receiver locations, respectively. Equation (1) is valid for arbitrarily anisotropic, heterogeneous media if the wavefield can be described within the framework of ray theory (Schleicher et al., 2001; Červený, 2001; Goldin, 1986).

In Paper I, equation (1) is combined with the Tsvankin-Thomsen (1994) nonhyperbolic moveout equation for the traveltime T to study the geometrical spreading of P-waves in a single horizontal orthorhombic layer. Both numerical modeling and analytic results reveal pronounced distortions of the geometrical spreading caused by the influence of polar and azimuthal anisotropy. Paper I demonstrates that the recovery of the reflection coefficient from the azimuthal AVO response is impossible without an accurate anisotropic geometrical-spreading correction (also, see Mallick et al., 1998).

The goal of this paper is to develop a practical implementation of the geometrical-spreading correction for layered azimuthally anisotropic media. The main emphasis of the paper is on models with orthorhombic symmetry considered as typical for naturally fractured reservoirs (e.g., Bakulin et al., 2000). It is clear from equation (1) that the key issue in computing the geometrical-spreading factor from surface data is to find a smooth approximation for reflection traveltime that can be used for a wide range of offsets and azimuths. We start by testing the accuracy of the simplified moveout equation introduced in Paper I for layered anisotropic media. While this equation provides a good fit to the traveltimes for media with a uniform orientation of the vertical symmetry planes, it requires modification when the symmetry-plane azimuths vary with depth.

After estimating the best-fit moveout coefficients using the nonhyperbolic semblance algorithm of Vasconcelos and Tsvankin (2004), we evaluate the traveltime derivatives with respect to offset and azimuth needed in equation (1). Numerical tests for layered orthorhombic models confirm that azimuthal anisotropy may produce comparable distortions in the geometrical spreading and in the reflection coefficient. The algorithm was also applied to wide-azimuth data collected at Weyburn field in Canada to generate the azimuthally varying geometrical-spreading factor for wide-angle reflections above the reservoir.

Moveout equation for orthorhombic media

The analysis in Paper I confirms the conclusion of Al-Dajani et al. (1998) that P-wave reflection traveltime in a horizontal orthorhombic layer with a horizontal symmetry plane is well-described by the Tsvankin-Thomsen (1994) nonhyperbolic moveout equation. The form of the equation remains the same for different anisotropic symmetries, but in the presence of azimuthal anisotropy the moveout coefficients become azimuthally dependent:

$$T^2(x,\alpha) = T_0^2 + \frac{x^2}{V_{\rm nmo}^2(\alpha)} + \frac{A_4(\alpha)\, x^4}{1 + A(\alpha)\, x^2}, \quad (2)$$

where x is the source-receiver offset, α is the azimuth of the source-receiver line, $V_{\rm nmo}$ is the normal-moveout (NMO) velocity, A_4 is the quartic moveout coefficient, and A is the coefficient that ensures the convergence of equation (2) for large source-receiver offsets.

The azimuthally varying NMO velocity traces out an ellipse with the axes parallel to the vertical symmetry planes of the orthorhombic layer (Grechka and Tsvankin, 1998):

$$V_{\rm nmo}^{-2}(\alpha) = \frac{\sin^2(\alpha-\phi)}{V_{\rm nmo}^{(1)}} + \frac{\cos^2(\alpha-\phi)}{V_{\rm nmo}^{(2)}}. \quad (3)$$

Here, $V_{\rm nmo}^{(1)}$ and $V_{\rm nmo}^{(2)}$ are the semi-minor and semi-major axes of the NMO ellipse, respectively, and ϕ is the azimuth of the semi-major axis with respect to the acquisition frame. Explicit expressions for the coefficients $A_4(\alpha)$ and $A(\alpha)$ for an orthorhombic layer are given in Al-Dajani et al. (1998) and Paper I.

The nonhyperbolic (x^4) term in equation (2) can be simplified by using an approximate equivalence between the P-wave kinematics in the vertical symmetry planes of orthorhombic and VTI (transversely isotropic with a vertical symmetry axis) media. As shown in Paper I, the VTI moveout equation of Alkhalifah and Tsvankin (1995) can be adapted for an orthorhombic layer by introducing an azimuthally varying anellipticity coefficient $\eta(\alpha)$ (Pech and Tsvankin, 2003):

$$T^2(x,\alpha) = T_0^2 + \frac{x^2}{V_{\rm nmo}^2(\alpha)} - \frac{2\eta(\alpha)\,x^4}{V_{\rm nmo}^2(\alpha)\,[T_0^2\,V_{\rm nmo}^2(\alpha) + (1+2\eta(\alpha))\,x^2]}, \qquad (4)$$

$$\eta(\alpha) = \eta^{(1)}\sin^2(\alpha-\phi) + \eta^{(2)}\cos^2(\alpha-\phi) - \eta^{(3)}\sin^2(\alpha-\phi)\cos^2(\alpha-\phi). \qquad (5)$$

The anellipticity parameters $\eta^{(1)}$, $\eta^{(1)}$, and $\eta^{(3)}$ are defined in the symmetry planes by analogy with the Alkhalifah-Tsvankin parameter η for VTI media (Grechka and Tsvankin, 1999b).

Numerical testing in Paper I proves that equation (4) provides a close approximation for P-wave moveout in a homogeneous orthorhombic layer. Below we apply equation (4) to more complicated, multilayered azimuthally anisotropic models.

Traveltime fitting for layered orthorhombic media

Models with uniform symmetry-plane orientation

Suppose the medium above the reflector is composed of horizontal layers with anisotropic symmetries no lower than orthorhombic, and the vertical symmetry planes in each layer have the same orientation. Note that in azimuthally isotropic (i.e., VTI or purely isotropic) layers any vertical plane is a plane of mirror symmetry. The uniform orientation of the symmetry planes in all layers implies that the model as a whole has two orthogonal vertical symmetry planes.

Because of the kinematic equivalence between the symmetry planes of orthorhombic and VTI media, P-wave nonhyperbolic moveout in the symmetry-plane directions is described by equation (4) with the effective parameter η computed from the VTI averaging equations (Tsvankin, 1997; 2001, Appendix 4B). Although for off-symmetry azimuthal directions the kinematic analogy with VTI media is valid only for weak anisotropy, the results of Paper I indicate that equation (4) parameterized by the best-fit values of $V_{\rm nmo}$ and η should still be sufficiently accurate. Therefore, the main issue in applying equation (4) to layered media with aligned symmetry planes is whether or not the azimuthal variation of the effective parameter $\eta(\alpha)$ can be described by the single-layer equation (5).

To estimate the effective moveout parameters in equation (4), we employ the 3D nonhyperbolic semblance algorithm of Vasconcelos and Tsvankin (2004). Wide-azimuth synthetic data are generated using ANRAY, the 3D anisotropic ray-tracing code developed by Gajewski and Pšenčík (1987). Vasconcelos and Tsvankin (2004) developed a three-step inversion procedure designed to make the multiparameter semblance search more efficient. First, conventional-spread data are used to reconstruct the NMO ellipse and evaluate the azimuth ϕ and the NMO velocities $V_{\rm nmo}^{(1)}$ and $V_{\rm nmo}^{(2)}$. Second, the anellipticity parameters $\eta^{(1)}$ and $\eta^{(2)}$, which are defined in the vertical symmetry planes, are estimated from the VTI nonhyperbolic semblance analysis in narrow sectors centered at the symmetry-plane directions. Third, the initial values of the parameters ϕ, $V_{\rm nmo}^{(1)}$, $V_{\rm nmo}^{(2)}$, $\eta^{(1)}$, and $\eta^{(2)}$ are used to specify the starting model for nonhyperbolic semblance search based on equations (4), (3), and (5).

Application of the algorithm to the four-layer model with the parameters listed in Table 1 confirms that equation (4) accurately describes long-spread moveout for the full range of azimuths. The model includes two orthorhombic layers with substantial magnitude of polar and azimuthal anisotropy sandwiched between two isotropic layers. As illustrated by Figure 1, the traveltimes computed from equation (4) with the inverted moveout parameters provide an excellent fit to the exact ray-traced traveltimes. The error of equation (4) does not exceed 0.3% of the zero-offset traveltime; similar results were obtained for a wide range of plausible orthorhombic models. The high accuracy of the traveltime fitting method, however, does not imply that the estimated parameters are close to the analytic values of the NMO velocities and the coefficient η because of the tradeoffs between various moveout coefficients (see Vasconcelos and Tsvankin, 2004). Nevertheless, as long as equation (4) is close to the exact traveltime, the moveout coefficients provide accurate input for the geometrical-spreading correction.

Models with misaligned symmetry planes

For media without throughgoing vertical symmetry planes, the azimuthal variation of the quartic moveout coefficient A_4 becomes more complicated and is described by five different trigonometric functions of the azimuth α (Al-Dajani et al., 1998). This implies that equation (5) for the azimuthally varying parameter η may no longer be accurate. However, extensive testing

	Layer 1	Layer 2	Layer 3	Layer 4
symmetry type	ISO	ORTH	ORTH	ORTH
V_{P0} (km/s)	1.5	2.437	3.0	3.2
thickness (km)	0.2	0.9	0.9	0.5
$\epsilon^{(1)}$	0	0.329	0.25	0
$\epsilon^{(2)}$	0	0.258	0.15	0
$\delta^{(1)}$	0	0.083	0.05	0
$\delta^{(2)}$	0	-0.078	-0.1	0
$\delta^{(3)}$	0	-0.106	0.15	0

Table 1. Parameters of a four-layer model (model 1) that includes two orthorhombic layers with aligned vertical symmetry planes $\alpha = 0°$ and $\alpha = 90°$.

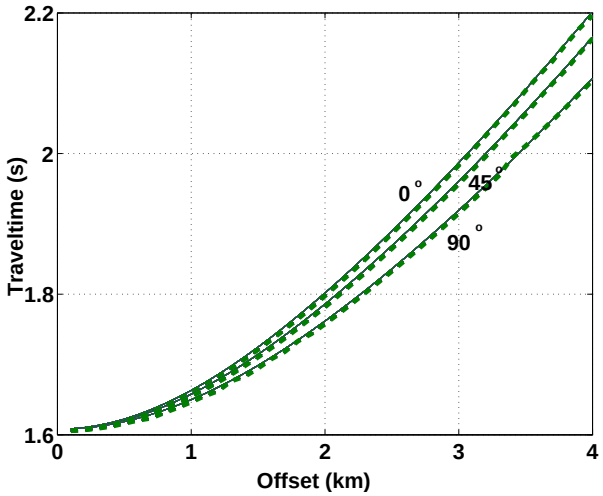

Figure 1. Accuracy of the traveltime fitting for the azimuths $\alpha = 0°$, $45°$, and $90°$ ($\alpha = 0°$ corresponds to one of the symmetry planes). The dashed line is the exact ray-traced traveltime, the solid line is the traveltime computed from equation (4) with the following estimated moveout parameters: $\phi = 90°$, $V_{\rm nmo}^{(1)} = 2.307$ km/s, $V_{\rm nmo}^{(2)} = 2.675$ km/s, $\eta^{(1)} = 0.305$, $\eta^{(2)} = 0.222$, and $\eta^{(3)} = -0.006$. The model parameters are listed in Table 1; the zero-offset reflection traveltime is $t_0 = 1.608$ s.

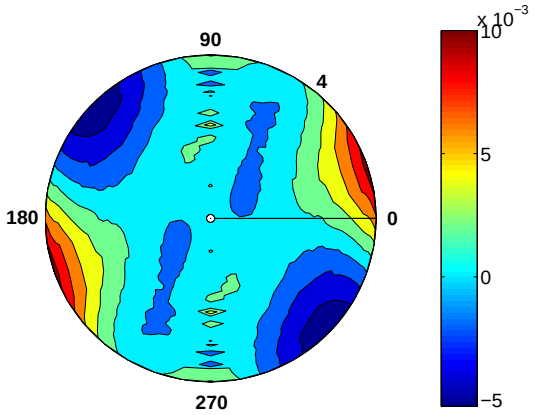

Figure 2. Map of the traveltime residuals (normalized by the zero-offset time) plotted as a function of offset and azimuth for a model with misaligned symmetry planes. The residuals are the differences between the best-fit traveltimes computed from equation (4) and the exact ray-traced times. The maximum offset is 4 km that corresponds to the offset-to-depth ratio of two. The estimated moveout parameters are $\phi = 78°$, $V_{\rm nmo}^{(1)} = 2.60$ km/s, $V_{\rm nmo}^{(2)} = 3.00$ km/s, $\eta^{(1)} = 0.567$, $\eta^{(2)} = 0.330$, and $\eta^{(3)} = 0.104$. The model parameters are listed in Table 2; the zero-offset traveltime $t_0 = 1.334$ s.

	Layer 1	Layer 2	Layer 3
symmetry type	ORTH	ORTH	ISO
V_{P0} (km/s)	3.0	3.0	3.2
thickness (km)	1.0	1.0	0.5
$\epsilon^{(1)}$	0.45	0.20	0
$\epsilon^{(2)}$	0.60	0.60	0
$\delta^{(1)}$	-0.15	0.15	0
$\delta^{(2)}$	-0.1	-0.15	0
$\delta^{(3)}$	0.2	-0.2	0

Table 2. Parameters for a three-layer model (model 2) that includes two orthorhombic layers with misaligned symmetry planes. The azimuth of the $[x_1, x_3]$ symmetry plane is $\phi = 45°$ in layer 1 and $\phi = 0°$ in layer 2.

that we performed for a range of orthorhombic models with misaligned symmetry planes shows that errors of equation (4) seldom exceed 0.5% of the zero-offset time. Apparently, the magnitude of the additional terms in the azimuthal dependence of η is relatively small, and the moveout inversion algorithm compensates for these missing terms by adjusting the best-fit parameters $\eta^{(1)}$, $\eta^{(2)}$, and $\eta^{(3)}$.

The model used in Figure 2 contains two orthorhombic layers with uncommonly strong polar and azimuthal anisotropy and the vertical symmetry planes misaligned by 45° (Table 2). For such an extreme example, the normalized errors of equation (4) reach 1%, which may be acceptable for purposes of moveout inversion, but not for geometrical-spreading correction. Indeed, errors in the traveltime function will be amplified during the computation of the first and second time derivatives that govern the geometrical-spreading factor [equation (1)].

Although models similar to the one in Figure 2 may not be typical, equation (4) can be modified in a relatively straightforward way to improve time fitting for multilayered media with misaligned symmetry planes. To introduce this modification, we analyze the effective parameter $\eta(\alpha)$ for a stack of horizontal orthorhombic layers by applying the VTI averaging equation (Tsvankin, 2001, equation 4.47) for each azimuth

α:

$$\eta(\alpha) = \frac{1}{8} \left\{ \frac{1}{V_{\rm nmo}^4(\alpha)\, t_0} \left[\sum_{i=1}^{N} (V_{\rm nmo}^{(i)}(\alpha))^4 \, (1 + 8\eta^{(i)}(\alpha))\, t_0^{(i)} \right] - 1 \right\}, \quad (6)$$

where $V_{\rm nmo}^{(i)}(\alpha)$ and $\eta^{(i)}(\alpha)$ are the interval parameters in layer i. Although equation (7) may become inaccurate for models with strong azimuthal anisotropy, it usually reproduces the shape of the azimuthal variation of the effective η (Al-Dajani et al., 1998).

Figure 3 shows a comparison between the parameter η computed from equation (7) (solid curve) and estimated by the moveout-inversion algorithm (dashed) for a two-layer orthorhombic model with misaligned symmetry planes. The shape of the two curves is quite similar, which explains the relatively low magnitude of the time residuals produced by equation (4). The misalignment of the symmetry planes, however, causes a rotation of the estimated η-curve with respect to the one calculated from equation (7).

The moveout-inversion algorithm cannot accommodate this rotation because the "principal axes" of the azimuthal variation of $\eta(\alpha)$ in equation (5) are parallel to the axes of the NMO ellipse [equation (3)]. Therefore, the traveltime fitting at far offsets can be improved by decoupling the nonhyperbolic moveout term from the NMO ellipse and introducing an additional angle ϕ_1 responsible for the azimuthal orientation of the effective parameter η:

$$\begin{aligned} \eta(\alpha) &= \eta^{(1)} \sin^2(\alpha - \phi_1) + \eta^{(2)} \cos^2(\alpha - \phi_1) \\ &- \eta^{(3)} \sin^2(\alpha - \phi_1) \cos^2(\alpha - \phi_1). \end{aligned} \quad (7)$$

The first two steps of the modified moveout-inversion algorithm remain the same as those described above, but at last step we fix the orientation of the NMO ellipse (angle ϕ) and search for the angle ϕ_1 and the other parameters using the full range of offsets and azimuths. Application of this algorithm to the model in Figure 2 results in a greatly improved time fitting (Figure 4) and a 15% increase in the semblance value for the best-fit model.

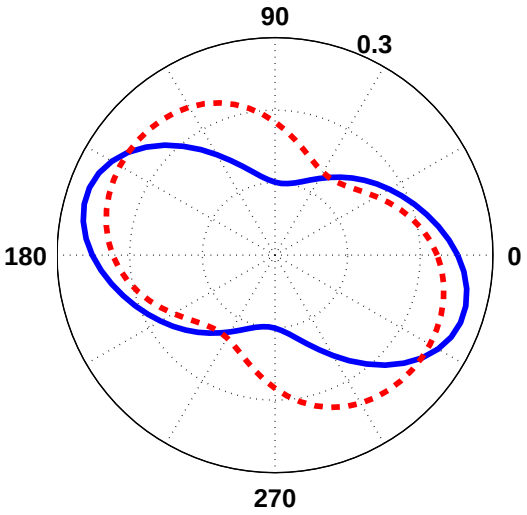

Figure 3. Comparison of the effective parameter $\eta(\alpha)$ computed from equation (7) (solid curve) and estimated by the inversion algorithm (dashed). The model is composed of two orthorhombic layers; for the top layer, $\phi = 15°$, $V_{P0} = 2.5$, $\epsilon^{(1)} = 0.2$, $\epsilon^{(2)} = 0.15$, $\delta^{(1)} = -0.1$, $\delta^{(2)} = 0.15$, and $\delta^{(3)} = 0.15$; for the bottom layer, $\phi = 0°$, $V_{P0} = 3.0$, $\epsilon^{(1)} = 0.15$, $\epsilon^{(2)} = 0.2$, $\delta^{(1)} = 0.15$, $\delta^{(2)} = -0.1$, $\delta^{(3)} = -0.15$.

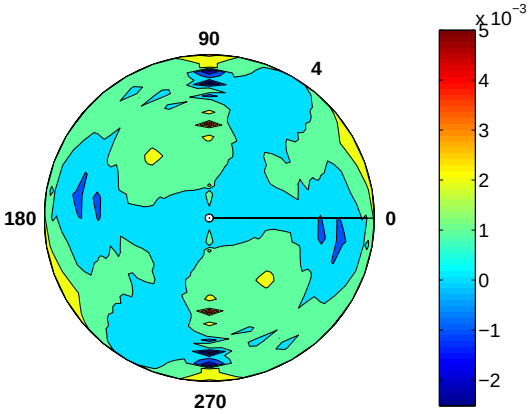

Figure 4. Same as Figure 2, but the traveltime fitting was performed using the modified inversion algorithm that allows for an independent orientation of the $\eta(\alpha)$–curve. The estimated parameters are $\phi = 81°$, $V_{\rm nmo}^{(1)} = 2.586$ km/s, $V_{\rm nmo}^{(2)} = 3.00$ km/s, $\eta^{(1)} = 0.594$, $\eta^{(2)} = 0.339$, $\eta^{(3)} = 0.161$, and $\phi_1 = 89°$.

Azimuth-dependent geometrical-spreading correction

The traveltime derivatives in the geometrical spreading equation (1) can be computed from the best-fit moveout parameters in equation (4). Explicit expressions for these derivatives are given in Paper I for the original form of the moveout equation with a single azimuthal angle ϕ. If the modified moveout equation provides a better fit to the traveltimes (e.g., a higher semblance value), the time derivatives can be easily rewritten using equation (7) for the parameter $\eta(\alpha)$.

The geometrical-spreading factor also depends on the group angles at the source (ϕ^s) and receiver (ϕ^r) locations, which are equal to each other for models with a horizontal symmetry plane. In most cases, the subsurface layer containing the source can be treated as isotropic and has a known P-wave velocity V. Then the angle ϕ^s can be computed using the ray parameter p estimated from the traveltime derivative dT/dx: $\sin\phi^s = pV$ (Ursin and Hokstad, 2003).

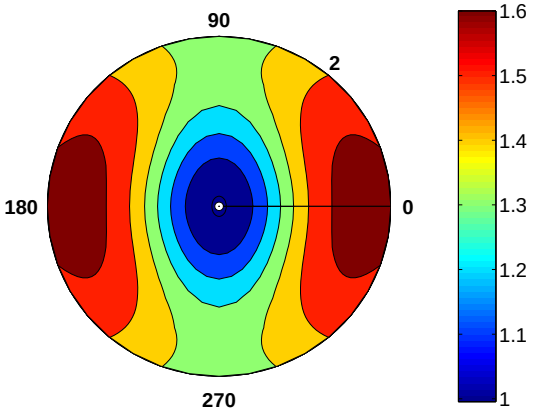

Figure 5. Plan view of the geometrical spreading for the reflection from the bottom of layer 3 in model 1 (Table 1). The factor L is normalized by its value in the reference isotropic homogeneous medium with $V_{\rm nmo} = (V^{(1)}_{\rm nmo} + V^{(2)}_{\rm nmo})/2$. The maximum offset-to-depth ratio is two.

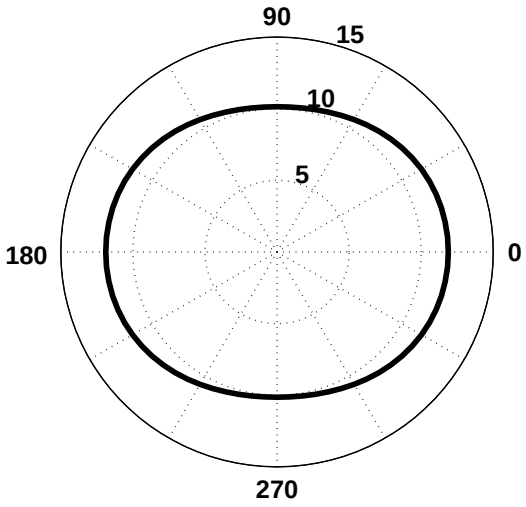

Figure 6. Azimuthally varying geometrical spreading for the reflection from the bottom of layer 3 in model 1 (Table 1) computed for an offset of 2 km. The corresponding phase incidence angle at the reflector is close to 30° (30° ± 5°).

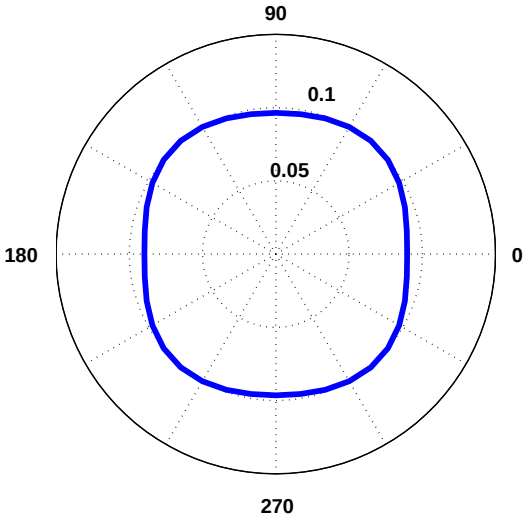

Figure 7. Azimuthally varying reflection coefficient from the bottom of layer 3 in model 1 (Table 1) computed for a phase incidence angle at the reflector of 30°.

Synthetic example

Using equation (4) with the inverted moveout parameters, we computed the geometrical-spreading factor for model 1. As was the case for a homogeneous orthorhombic medium discussed in Paper I, the influence of anisotropy leads to pronounced, azimuthally-dependent distortions of the geometrical spreading (Figure 5). For example, the factor L for the reflection from the bottom of layer 3 decreases by 17% between the azimuths $\alpha = 0°$ and 90° (Figure 6; the offset is close to the reflector depth). The reflection coefficient for this event, however, increases by only 12.6% over the same azimuthal range. Since all layers are horizontal, the dependence of the geometrical spreading on azimuth is caused entirely by the azimuthal anisotropy above the reflector. Clearly, if the anisotropic geometrical spreading is unaccounted for, it can completely compromise the azimuthal AVO signature for this model.

The high accuracy of our algorithm is verified by the comparison with the results of dynamic ray tracing (using code ANRAY) for model 1 in Figure 8. The geometrical-spreading factors computed by the two methods are almost identical for offset-to-depth ratios less than 1.5, and only slightly diverge at longer offsets. The deviation of our result from that of the ray tracing, which reaches 8% for an azimuth of 0°, can be explained by small errors in the traveltime fitting. Nevertheless, our method produces a sufficiently close approximation to the ray-traced geometrical-spreading factor for a wide range of offsets and azimuths.

Field-data application

To demonstrate the influence of azimuthal anisotropy on the geometrical spreading for field data, we applied the algorithm to wide-azimuth reflection events acquired above a fractured reservoir at Weyburn field in Canada by the Reservoir Characterization Project (a research consortium at CSM). Vasconcelos and Tsvankin (2004) carried out nonhyperbolic moveout inversion for P-wave reflections from several interfaces in the overburden and obtained relatively large values of the parameters $\eta^{(1,2,3)}$ reaching 0.25. They also concluded that at least the shallow part of the overburden exhibits non-negligible azimuthal anisotropy. The results of Vasconcelos and

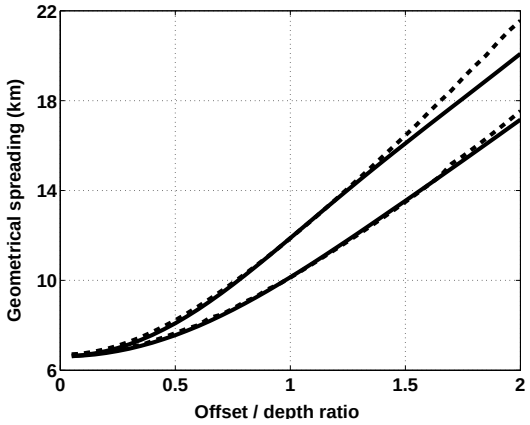

Figure 8. Accuracy of our method for the reflection from layer 3 in model 1; the azimuths are $\alpha = 0°$ and $90°$. The factor L is computed from dynamic ray tracing (dashed line) and our algorithm (solid).

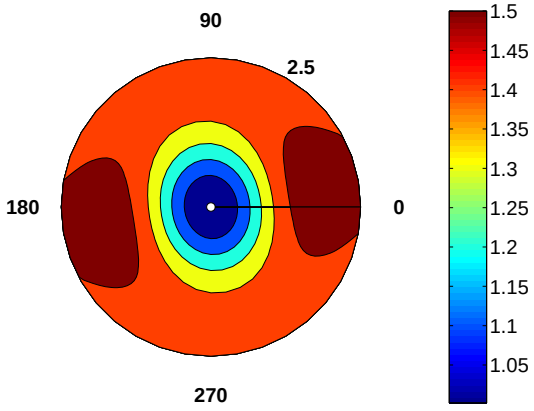

Figure 9. Plan view of the normalized geometrical spreading for the P-wave reflection from the Mississippian formation (the top of the reservoir) at Weyburn field computed for CMP 10829. The factor L is normalized by its value in the reference isotropic homogeneous medium with $V_{\rm nmo} = (V_{\rm nmo}^{(1)} + V_{\rm nmo}^{(2)})/2$. The moveout parameters are taken from Vasconcelos and Tsvankin (2004): $\phi = 99°$, $V_{\rm nmo}^{(1)} = 2.371$ km/s, $V_{\rm nmo}^{(2)} = 2.464$ km/s, $\eta^{(1)} = 0.255$, $\eta^{(2)} = 0.186$, and $\eta^{(3)} = -0.062$. The depth of the reflector is 1.4 km (the maximum offset-to-depth ratio is 2.5).

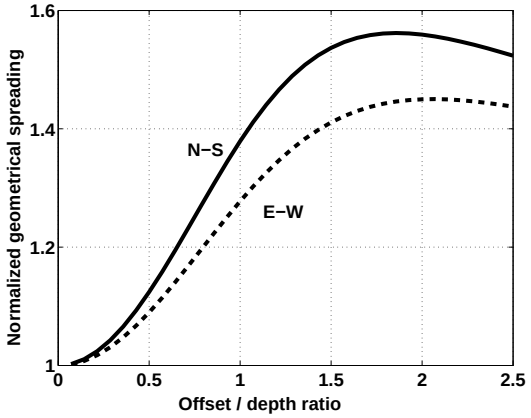

Figure 10. Normalized geometrical spreading for the reflection from the Mississippian formation computed in the east-west and north-south directions for CMP 10829.

Tsvankin (2004) are in good agreement with the analysis of shear-wave splitting by Cardona (2002) and of the azimuthal AVO response by Jenner (2001).

In particular, Jenner (2001) found that the P-wave AVO attributes at the reservoir level vary with azimuth. His amplitude processing, however, included only the conventional geometrical-spreading correction for isotropic media. To evaluate possible distortions of the AVO response caused by the influence of anisotropy on the geometrical spreading, we applied our algorithm to the reflection from the top of the reservoir (Figure 9). The moveout parameters were obtained by Vasconcelos and Tsvankin (2004) using the original equation (4) with a single azimuthal angle ϕ.

A plan view of the normalized geometrical-spreading factor in the overburden is displayed in Figure 9. The influence of anisotropy causes a dramatic 50% distortion in the geometrical spreading for offset-to-depth ratios close to two. The magnitude of the azimuthal variation of the factor L at far offsets reaches 10% (Figure 10). Such a difference between the geometrical spreading in the east-west and north-south directions is sufficiently large to cause distortions in the azimuthal variation of the AVO gradient studied by Jenner (2001).

Discussion and conclusions

The formalism suggested in Paper I (Xu et al., 2003) for describing the geometrical spreading of reflected waves is used here to develop a practical methodology for the P-wave geometrical-spreading correction in layered azimuthally anisotropic media. The correction, which involves the spatial derivatives of the reflection traveltime and the group-velocity vector at the source location, does not require knowledge of the velocity model. If the layer containing the source is isotropic, the group angle can be estimated in a straightforward way from the slope of the traveltime curve. Hence, the main issue in computing the geometrical-spreading factor from surface data is to find a sufficiently accurate, smooth approximation for wide-azimuth, long-offset reflection moveout in the presence of azimuthal anisotropy.

Numerical testing shows that even for models composed of strongly anisotropic orthorhombic layers, long-spread P-wave reflection traveltime can be accurately described by a nonhyperbolic moveout equation that has the same form as the widely used Alkhalifah-

Tsvankin (1995) equation for VTI media. To accommodate the influence of azimuthal anisotropy, both moveout parameters - the NMO velocity $V_{\rm nmo}$ and the anellipticity coefficient η - have to vary with azimuth α. While $V_{\rm nmo}(\alpha)$ traces out an ellipse in media of almost any complexity (Grechka and Tsvankin, 1998), the form of the function $\eta(\alpha)$ depends on the degree of alignment of the symmetry planes in the constituent layers.

If the vertical symmetry planes have the same azimuths in all layers, then the model as a whole has two orthogonal symmetry planes, and the azimuthal dependence of η is given by the equation for a homogeneous orthorhombic medium discussed by Pech and Tsvankin (2003) and in Paper I. For purposes of geometrical-spreading correction, such a model is fully equivalent to a single orthorhombic layer. In this case, the moveout equation is controlled by the azimuth ϕ of one of the symmetry planes, two symmetry-plane NMO velocities $V_{\rm nmo}^{(1,2)}$, and three anellipticity parameters $\eta^{(1,2,3)}$ that govern $\eta(\alpha)$. To estimate the six moveout parameters, we use the algorithm of Vasconcelos and Tsvankin (2004) based on a 3D nonhyperbolic semblance operator.

For models with depth-varying orientation of the symmetry planes, the azimuthal variation of the effective parameter η is no longer tied to the axes of the NMO ellipse. We show that the accuracy of the moveout equation can be maintained by simply introducing an additional azimuthal angle ϕ_1 that determines the direction of the "principal axes" of the function $\eta(\alpha)$. Keeping the same general form of the moveout equation for azimuthally anisotropic and VTI media helps to facilitate the transition between models with different symmetries in both the moveout inversion and geometrical-spreading correction.

Synthetic tests for layered orthorhombic media illustrate the high sensitivity of the spatially varying geometrical spreading to the anisotropic parameters. The magnitude of the anisotropy-induced azimuthal variation of the geometrical spreading may exceed the relative difference between the reflection coefficients in the symmetry planes.* Therefore, anisotropic geometrical-spreading correction should become an integral part of azimuthal AVO inversion.

The importance of correcting wide-azimuth data for geometrical spreading prior to AVO analysis was highlighted by applying the algorithm to field data acquired at Weyburn field in Canada. The geometrical-spreading factor for the reflection from the top of the fractured reservoir is influenced by the ellipticity of the NMO-velocity function and, especially, by the large values (exceeding 0.2) of the effective parameters $\eta^{(1,2,3)}$. The reliability of the AVO attributes studied by Jenner (2001) can be improved by taking into account the variation of the geometrical spreading between the east-west and north-south directions.

*Comparisons of this type, however, strongly rely on the model assumptions because the geometrical spreading of reflected waves is independent of the elastic parameters beneath the reflector.

Acknowledgments

We are grateful to Ed Jenner (GMG/Axis) and Tom Davis (CSM) for providing the Weyburn data set to the Center for Wave Phenomena (CWP) and to Ivan Vasconcelos (CSM) for making available to us his moveout inversion code and processing results. The support for this work was provided by the Consortium Project on Seismic Inverse Methods for Complex Structures at CWP and by the Chemical Sciences, Geosciences and Biosciences Division, Office of Basic Energy Sciences, U.S. Department of Energy.

References

Al-Dajani, A., Tsvankin, I., and Toksöz, M. N., 1998, Nonhyperbolic reflection moveout for azimuthally anisotropic media: 68th Ann. Internat. Mtg., Soc. Expl. Geophys., Expanded Abstracts, 1479–1482.

Alkhalifah, T., and Tsvankin, I., 1995, Velocity analysis for transversely isotropic media: Geophysics, **60**, 1550–1566.

Bakulin, A., Grechka, V., and Tsvankin, I., 2000, Estimation of fracture parameters from reflection seismic data – Part II: Fractured models with orthorhombic symmetry: Geophysics, **65**, 1803–1817.

Cardona, R., 2002, Fluid substitution theories and multicomponent seismic characterization of fractured reservoirs: PhD thesis, Colorado School of Mines.

Červený, V., 2001, Seismic ray theory: Cambridge University Press.

Gajewski, D., and Pšenčík, I., 1987, Computation of high frequency seismic wavefields in 3-D laterally inhomogeneous anisotropic media: Geophys. J. R. Astr. Soc., **91**, 383–412.

Goldin, S., 1986, Seismic traveltime inversion: Society of Exploration Geophysics.

Grechka, V., and Tsvankin, I., 1998, 3-D description of normal moveout in anisotropic inhomogeneous media: Geophysics, **63**, 1079–1092.

Grechka, V., and Tsvankin, I., 1999a, 3-D moveout inversion in azimuthally anisotropic media with lateral velocity variation: Theory and a case study: Geophysics, **64**, 1202–1218.

Grechka, V., and Tsvankin, I., 1999b, 3-D moveout velocity analysis and parameter estimation for orthorhombic media: Geophysics, **64**, 820–837.

Hall, S., and Kendall, J.M., 2003, Fracture characterization at Valhall: application of P-wave amplitude variation with offset and azimuth (AVOA) analysis to a 3-D ocean-bottom data set: Geophysics, **68**, 1150–1160.

Jenner, E., 2001, Azimuthal anisotropy of 3-D compressional wave seismic data, Weyburn field, Saskatchewan, Canada.: PhD theis, Colorado School of Mines.

Lynn, H.B., Campagna, D., Simon, K.M., and Beckham, W.E., 1999, Relationship pf P-wave seismic attributes, azimuthal anisotropy, and commercial gas pay in 3-D P-wave multiazimuth data, Rulison Field, Piceance Basin, Colorado: Geophysics, **64**, 1312–1328.

Mallick, S., Craft, K., and Meister, L., 1998, Determination of the principal directions of azimuthal anisotropy from P-wave seismic data: Geophysics, **63**, 692–706.

Maultzsch, S., Horne, S., Archer, S., and Burkhardt, H., 2003, Effects of an anisotropic overburden on azimuthal amplitude analysis in horizontal transverse isotropic media: Geophysics Prospecting, **51**, 61–74.

Pech, A., and Tsvankin, I., 2003, Quartic moveout coefficient for a dipping azimuthally anisotropic layer: CWP Annual Project Review (CWP-452), 133–142, (also Geophysics, in print).

Rüger, A., 2001, Reflection coefficients and azimuthal AVO analysis in anisotropic media: Society of Exploration Geophysics.

Schleicher, J., Tygel, M., Ursin, B., and Bleistein, N., 2001, The Kirchhoff-Helmholtz integral for anisotropic elastic media: Wave Motion, **34**, 353–364.

Tsvankin, I., and Thomsen, L., 1994, Nonhyperbolic reflection moveout in anisotropic media: Geophysics, **59**, 1290–1304.

Tsvankin, I., 1995, Body-wave radiation patterns and AVO in transversely isotropic media: Geophysics, **60**, 1409–1425.

Tsvankin, I., 1997, Anisotropic parameters and P-wave velocity for orthorhombic media: Geophysics, **62**, 1292–1309.

Tsvankin, I., 2001, Seismic signatures and analysis of reflection data in anisotropic media: Elsevier Science Publ. Co., Inc.

Ursin, B., and Hokstad, K., 2003, Geometrical spreading in a layered transversely isotropic medium with vertical symmetry axis: Geophysics, **68**, 2082–2091.

Vasconcelos, I., and Tsvankin, I., 2004, Nonhyperbolic moveout inversion of P-waves in azimuthally anisotropic media: Algorithm and application to field data: CWP Annual Project Review.

Xu, X., Tsvankin, I., and Pech, A., 2003, Geometrical spreading of reflected waves in azimuthally anisotropic media: CWP Annual Project Review (CWP-447), 37–47, (also submitted to Geophysics).